Eur. Phys. J. D (2013)
DOI: 10.1140/epjd/e2013-40165-7

THE EUROPEAN PHYSICAL JOURNAL D

Regular Article

Nonlinear pulsational eigenmodes of a planar collisional dust molecular cloud with grain-charge fluctuation

P.K. Karmakar[a] and B. Borah

Department of Physics, Tezpur University, Napaam-784028, Tezpur, Assam, India

Received 24 March 2013 / Received in final form 14 June 2013
Published online (Inserted Later) – © EDP Sciences, Società Italiana di Fisica, Springer-Verlag 2013

Abstract. We try to present a theoretical evolutionary model leading to the excitations of nonlinear pulsational eigenmodes in a planar (1D) collisional dust molecular cloud (DMC) on the Jeans scale. The basis of the adopted model is the Jeans assumption of self-gravitating homogeneous uniform medium for simplification. It is a self-gravitating multi-fluid consisting of the Boltzmann distributed warm electrons and ions, and the inertial cold dust grains with partial ionization. Dust-charge fluctuations, convections and all the possible collisions are included. The grain-charge behaves as a dynamical variable owing mainly to the attachment of the electrons and ions to the grain-surfaces randomly. The adopted technique is centered around a mathematical model based on new solitary spectral patterns within the hydrodynamic framework. The collective dynamics of the patterns is governed by driven Korteweg-de Vries (d-KdV) and Korteweg-de Vries (KdV) equations obtained by a standard multiscale analysis. Then, simplified analytical and numerical solutions are presented. The grain-charge fluctuation and collision processes play a key role in the DMC stability. The sensitive dependence of the eigenmode amplitudes on diverse relevant plasma parameters is discussed. The significance of the main results in astrophysical, laboratory and space environments are concisely summarized.

1 Introduction

The most important ingredient of the inter-stellar medium (ISM) is solid matter of dust grains dispersed in gaseous phase of background plasma [1–3]. The dimension of the dust grains, composed mainly of graphite, silicate and metallic compound, vary from micron to sub-micron scale size [1–4]. In regions of the self-gravitating ISM that are sufficiently dense, and well-shielded against the dissociating effects of interstellar ultraviolet radiation, hydrogen atoms bind to form molecules. Star and cluster formation normally occur exclusively within this molecular phase of the ISM through self-gravitational collapse. This region of the ISM called dust molecular cloud (DMC) has always been well-known to be the best site of star formation through the Jeans instability [1–5]. Thus, the self-gravitational breakdown of the grains in such clouds plays a crucial key role in the formation processes of stars, galactic structures, planetary bodies, clusters and their evolutions as a whole [1–10].

In the clouds, the grains acquire a non-negligible electric charge due to interstellar radiation fields ionizing the background gas, resulting in sticking plasma collision effects (surface bombardment with the plasma electrons and ions), and some other high-energetic mechanisms [11–22]. In other words, the grain acquires charge by capturing electrons and ions from the background plasma, while, the grain looses charge by emitting photoelectrons induced by UV photons [4,15–19]. The static electrical capacitor charging model of the spherical grains normally adopted may be found to be quite idealistic. The grain charge $q_d = Z_d e$, indeed, may fluctuate [11–22]. It may, for example, fluctuate between $\pm 1e$ and 0 in the cold (dark) clouds at $T < 30$ K. Again, $q_d > 100e$ in the HII region, where $T \sim 10^4$ K [11]. As the dusty plasma system oscillates around its defined equilibrium, q_d fluctuates about its equilibrium value like a source, or sink [19,20]. As a consequence, novel collective features to the normal dusty plasma behavior in diverse situations are thereby introduced in practical situations both with [11,19–21] and without [13–16] self-gravity.

Investigation of various waves, instabilities and fluctuations supported in such DMCs and like giant atmospheres has become an emerging problem in space and astrophysical environments of present-day research interest because of their elementary roles played in understanding self-gravitational collapse, formation and evolution of galactic evolution [1–10]. The existence of both linear [5,10,11] and nonlinear [5–9,21–24] gravito-electrostatic eigenmodes under static grain charging model has been studied by many authors in the past. Pandey et al. [11] have studied pulsational mode stability in DMCs with dust-charge fluctuations. The fluctuations in the grain-charges are due basically to capture or liberation of additional electrons

[a] e-mail: pkk@tezu.ernet.in

and ions (or protons), which lead to density and momentum losses, or even gains [11–20]. This acts as a source of wave damping, or growth. Several frequency regimes of observations are judiciously possible under such charge fluctuations in linear modes [11–22]. If the dust charging is slow compared to the wave fluctuations, the dust charges are treated as constant. On the other hand, when charge and wave fluctuations occur on comparable timescales, then wave damping or growth occurs at the linear level, and no reasonable nonlinear evolution can thereby be affected. Most interesting investigation may be an intermediate regime, where the linear waves are not affected, but the dust charging influences the slower nonlinear eigenmode developments on the observational scales of space and time. As a result, the variation of charge on the grains introduces an additional temporal scale in plasma. Thus, the fluctuating grain charge becomes a new dynamical variable evolving in time, which in turn, affects the wave-activity spectra supported in such a broad class of complex plasma systems [11–31].

In this communication, we try to propose an idealized theoretical model to show the basic features of the nonlinear gravito-electrostatic eigenmodes (pulsational type) supported in a simplified field-free planar (1D) DMC. The main motivation is to examine the nature of the nonlinear fluctuations associated with the charge-varying cloud model. The adopted model is similar to that as considered by Pandey et al. [11] describing the linear eigenmode counterparts only. However, for simplicity, the governing equations for the description of the thermal species are taken directly from various works already done by many authors on self-gravitating collisional plasma in the past [10,12,26–28]. An additional stimulus for considering this kind of model is that it depicts the realistic picture of astrophysical relevance in an abridged manner. We apply a standard methodology of multiple scaling techniques [6,14,16] around the defined gravito-electrostatic equilibrium over the basic cloud structure equations. It is found that the nonlinear electrostatic fluctuations dynamically evolve like a driven Korteweg-de Vries (d-KdV) equation with a unique self-consistent nonlinear driving source, and the self-gravitational fluctuations are governed by a new Korteweg-de Vries (KdV) equation with no such source. A detailed multi-parameter numerical analysis as initial value problems by the fourth-order Runge-Kutta method under some judicious plasma conditions is carried out. The gravito-electrostatic eigenmode structures in the astrophysical grainy plasma appear mainly in the form of new solitary spectral patterns, which are shown subsequently to have realistic astrophysical significance and applicability in newer perspectives.

Apart from the "introduction" part described in Section 1 above, this paper is structurally organized in a usual simple format as follows. Section 2 contains physical model of the plasma system under investigation. Section 3 contains the basic governing equations describing the DMC structure. Section 4 contains analytical calculation scheme for the derivation of nonlinear evolution equations describing eigenmode excitations. Section 5 shows the numerical calculation scheme displaying the graphical constructs of the eigenmodes. Section 6 includes the relevant results and discussions. Lastly and most importantly, Section 7 portrays the main conclusions of scientific interest and astrophysical applicability along with some highlighted future directions.

2 Physical model

A simplified field-free planar one-dimensional (1D) DMC is considered under hydrodynamic equilibrium configuration with presumed global quasi-neutrality. This is well-known that the DMC equilibrium cannot be assumed like a truly homogeneous one, it must be derived from the governing structure equations themselves. Still, for simplicity, hydrodynamic considerations are made to apply the conventional fluid equations in our investigation in presence of self-gravity contributed by the heavier grains. The considered planar 1D geometry is considered to be equivalent to a spherical symmetry, wherein, the fluctuations propagate in radial direction only. This is how the spherical (3D) problem gets transformed into a simplified planar (1D) problem. Such a model could be visualized as the static distribution of the multi-fluid consisting of electrons, ions, neutral gas, and neutral dust grains along with partial ionization. The solid matter of the spherical dust grains is embedded in the gaseous phase of the background quasi-neutral plasma on the astrophysical scale. The grains get, as usual, electrically charged due basically to the plasma environment amid statistically random sticking collision processes [13–19]. All the grains, for mathematical simplicity, are assumed to be of identical nature having the same geometrical size, so that all the charged grains (hotter than the neutral grains) contain the same amount of equilibrium charge in the defined plasma environment. This is in accordance with spherical capacitor charging model of the spherical grains [16–20]. The grain-size is much smaller than the inter-grain separation, which is lesser than the plasma Debye length. The actual grain charge included in the model, in reality, fluctuates and evolves dynamically due to the attachment phenomena of the thermal plasma species to the grain surface.

This may be pertinent to add furthermore that the model setup sustains nonlinearity due to fluidity, dispersion due to self-gravity within planar geometrical curvature and dissipation due to collective collisional dynamics of intrinsic cloud origin. The strength of the electric forces developed due to space-charge polarization effects (local charge imbalance) are taken to be too weak to excite higher order contributions of the various nonlinear terms on the Jeans scale, thereby validating our underlying assumption of weak nonlinearity.

In normal DMCs, magnetic field is $\sim$1 μG, around which the charged grains, in principle, perform gyration [11]. For $q_d \sim 100e$ and $m_d \sim 10^{-13}$ kg, the gyro-period of the charged grains is $\tau_{cd} \sim 10^6$ years, which is too slow to influence the grainy fluctuation dynamics considerably. The effects of the magnetic field on the grains are experienced through the plasma particles, which are

usually well coupled to the field. The effect of the magnetic field is ignored, and an unmagnetized configuration is considered [11]. The dust-charge fluctuations, furthermore, are taken into account to see the modified nonlinear eigenmode spectra. A considered wide-range spectrum in the grain-mass ($m_d \sim 10^{-8}$–10^{-18} kg) physically allows a suitable parameter regime, where the unipolar self-gravitational and bipolar electrostatic forces may become comparable. Thus, the joint interplayed action of the two opposing forces in establishing gravito-electrostatic equilibrium may play an important role in the formation processes of equilibrium stellar structures. Moreover, all the possible collisional dynamics and effects are included in the calculation scheme. The lighter constituents like the electrons and ions are considered as the thermal species (Boltzmannian); and the charged and neutral spherical heavier grains are treated as the inertial species (hydrodynamic fluid) for any observation on the Jeans scales of space and time. A bulk uniform flow is assumed to preexist in the equilibrium. The efficacious cloud mass, as a whole, is collectively contributed by the heavier inertial grains, but within the validity limit of the Newtonian point-mass approximation [8,9]. It may be pertinent to add further that high collisional momentum exchange from the plasma species to the gains may thermalize the complex plasma with the neutral grains. However, the drag effects and other force field effects are neglected for the time being. For additional simplicity and idealization in calculation, we neglect the presence of rotation, viscosity, circulation, spatio-temporal inhomogeneities, grain-size distribution, etc.

3 Basic governing equations

The cloud equilibrium is a quasi-static distribution of the multi-fluid constituent particles in quasi-neutral hydrodynamic equilibrium. The light neutral gas particles develop a constant background, which is weakly coupled to the collapsing charged grains. We model the fluctuation dynamics by the normal continuity [26–28]; but with collisional momentum, and coupling electro-gravitational Poisson equations described with all conventional notations on the astrophysical scale [8–12]. Thus, the electron dynamical evolution is portrayed (in unnormalized form) as follows:

$$\frac{\partial n_e}{\partial t} + n_e \frac{\partial v_e}{\partial x} + v_e \frac{\partial n_e}{\partial x} = 0, \tag{1}$$

and

$$T_e \frac{\partial n_e}{\partial x} + e n_e \frac{\partial \phi}{\partial x} + m_e n_e f_{edc} v_e = 0. \tag{2}$$

The dynamical evolution of the plasma ions composing the DMC is, similarly, governed by:

$$\frac{\partial n_i}{\partial t} + n_i \frac{\partial v_i}{\partial x} + v_i \frac{\partial n_i}{\partial x} = 0, \tag{3}$$

and

$$T_i \frac{\partial n_i}{\partial x} + e n_i \frac{\partial \phi}{\partial x} + m_i n_i f_{idc} v_i = 0. \tag{4}$$

As we are interested in weakly nonlinear low-frequency eigenmodes, the inertial terms in equations (2) and (4) signifying the force (density) balances are neglected. Here, f_{edc} and f_{idc} are the electron-charged dust and ion-charged dust collision frequencies in unnormalized form, respectively. Also, the electrons and ions have population densities n_e, n_i; velocities v_e, v_i; masses m_e, m_i; charges $-e$, $+e$; and temperatures T_e, T_i such that $T_e \approx T_i = T_p$ (in eV); respectively. Thus, the thermodynamics of the electrons and ions are governed by their isothermal equations of state on their thermal pressures, $p_e = n_e T_e$ and $p_i = n_i T_i$, correspondingly. In addition, ϕ represents the electrostatic potential (due to space-charge polarization). Accordingly, the neutral and charged grain evolutions in the configuration space coordinatized by (x, t) are, respectively, described by the following fluid equations,

$$\frac{\partial n_{dn}}{\partial t} + n_{dn} \frac{\partial v_{dn}}{\partial x} + v_{dn} \frac{\partial n_{dn}}{\partial x} = 0, \tag{5}$$

$$m_{dn} n_{dn} \left[\frac{\partial v_{dn}}{\partial t} + v_{dn} \frac{\partial v_{dn}}{\partial x} \right] = -T_p \frac{\partial n_{dn}}{\partial x} - m_{dn} n_{dn} \frac{\partial \psi}{\partial x} - m_{dn} n_{dn} f_{nc} \left(v_{dn} - v_{dc} \right), \tag{6}$$

$$\frac{\partial n_{dc}}{\partial t} + n_{dc} \frac{\partial v_{dc}}{\partial x} + v_{dc} \frac{\partial n_{dc}}{\partial x} = 0, \tag{7}$$

and

$$m_{dc} n_{dc} \left[\frac{\partial v_{dc}}{\partial t} + v_{dc} \frac{\partial v_{dc}}{\partial x} \right] = -T_p \frac{\partial n_{dc}}{\partial x} - q_d n_{dc} \frac{\partial \phi}{\partial x} - m_{dc} n_{dc} \frac{\partial \psi}{\partial x} - m_{dc} n_{dc} f_{cn} \left(v_{dc} - v_{dn} \right). \tag{8}$$

The spatial distributions of the electrostatic potential (ϕ) and self-gravitational potential (ψ) are defined by the combining Poisson equations thereby closing the model as given below,

$$\frac{\partial^2 \phi}{\partial x^2} = -4\pi \left[e \left(n_i - n_e \right) - q_d n_{dc} \right], \tag{9}$$

and

$$\frac{\partial^2 \psi}{\partial x^2} = 4\pi G \left(m_{dn} n_{dn} + m_{dc} n_{dc} - m_d n_{d0} \right), \tag{10}$$

where, $n_{d0} = n_{dc0} + n_{dn0}$ models the Jeans swindle [8–12] of the equilibrium unipolar gravitational force field, which provides a formal justification for discarding the unperturbed gravitational field. Indeed, a spatially homogeneous self-gravitating plasma system cannot be in static equilibrium (for which $\partial^2 \psi / \partial \xi^2 \sim 0$), since there is no pressure gradient to balance the gravitational force (originating from the equilibrium cloud-material distribution $m_{dn} n_{dn} + m_{dc} n_{dc} \approx m_d n_{d0}$ as evident from Eq. (10)). This physically means that self-gravitational potential is sourced only by density fluctuations of the infinite uniform homogeneous background medium under consideration [32]. The Jeans assumption (ad hoc) for the self-gravitating uniform homogeneous medium may not be

the most suitable one, but it allows us to treat the self-gravitating inhomogeneous plasma dynamics analytically in a simplified way [32]. The results (on fluctuations and eigenmodes) based on this homogenization assumption in most of the cases have been found to be not far from realistic picture [5,6,21,32]. Finally, the charge dynamics equation [11] for the variable-charge grains is given by:

$$\frac{\partial q_d}{\partial t}+v_{dc}\frac{\partial q_d}{\partial x}=e\left[f_{ed}\frac{(n_e-n_{e0})}{n_{d0}}-f_{id}\frac{(n_i-n_{e0})}{n_{d0}}\right], \quad (11)$$

where, f_{ed} and f_{id} are electron-dust and ion-dust collision frequencies, respectively. Here, G (=6.67 $\times$ 10^{-11} N m^2 kg^{-2}) represents the universal gravitational constant. Furthermore, the neutral and charged grains each with mass m_d and temperature T_d have population densities n_{dn}, n_{dc}; and velocities v_{dn}, v_{dc}; respectively.

4 Analytical calculation scheme

In order to investigate the nonlinear gravito-electrostatic fluctuations supported in the cloud analytically as a first step, we apply a standard normalization procedure of astrophysical relevance [9] to obtain the normalized form of equations (1)–(11), respectively, given as follows:

$$\frac{\partial N_e}{\partial \tau}+N_e\frac{\partial M_e}{\partial \xi}+M_e\frac{\partial N_e}{\partial \xi}=0, \quad (12)$$

$$\frac{\partial N_e}{\partial \xi}+N_e\frac{\partial \Phi}{\partial \xi}+\left(\frac{m_e}{m_d}\right)N_eM_eF_{edc}=0, \quad (13)$$

$$\frac{\partial N_i}{\partial \tau}+N_i\frac{\partial M_i}{\partial \xi}+M_i\frac{\partial N_i}{\partial \xi}=0, \quad (14)$$

$$\frac{\partial N_i}{\partial \xi}+N_i\frac{\partial \Phi}{\partial \xi}+\left(\frac{m_i}{m_d}\right)N_iM_iF_{idc}=0, \quad (15)$$

$$\frac{\partial N_{dn}}{\partial \tau}+N_{dn}\frac{\partial M_{dn}}{\partial \xi}+M_{dn}\frac{\partial N_{dn}}{\partial \xi}=0, \quad (16)$$

$$N_{dn}\left[\frac{\partial M_{dn}}{\partial \tau}+M_{dn}\frac{\partial M_{dn}}{\partial \xi}\right]=-\frac{1}{n_{dn0}}\frac{\partial N_{dn}}{\partial \xi}$$
$$-\left(\frac{m_{dn}}{n_{dn0}e}\right)N_{dn}\frac{\partial \Psi}{\partial \xi}-\left(\frac{1}{n_{dn0}}\right)F_{nc}\left(M_{dn}-M_{dc}\right), \quad (17)$$

$$\frac{\partial N_{dc}}{\partial \tau}+N_{dc}\frac{\partial M_{dc}}{\partial \xi}+M_{dc}\frac{\partial N_{dc}}{\partial \xi}=0, \quad (18)$$

$$N_{dc}\left[\frac{\partial M_{dc}}{\partial \tau}+M_{dc}\frac{\partial M_{dc}}{\partial \xi}\right]=-\frac{1}{n_{dc0}}\frac{\partial N_{dc}}{\partial \xi}$$
$$-\left(\frac{q_d}{n_{dc0}}\right)Q_dN_{dc}\frac{\partial \Phi}{\partial \xi}-\left(\frac{m_{dc}}{n_{dc0}e}\right)N_{dc}\frac{\partial \Psi}{\partial \xi}$$
$$-\left(\frac{1}{n_{dc0}}\right)F_{cn}\left(M_{dc}-M_{dn}\right), \quad (19)$$

$$\frac{\partial^2 \Phi}{\partial \xi^2}=\frac{e}{m_{dc}^2n_{d0}G}$$
$$\times\left[e\left(n_{e0}N_e-n_{i0}N_i\right)+\left(q_{d0}n_{dc0}\right)Q_dN_{dc}\right], \quad (20)$$

$$\frac{\partial^2 \Psi}{\partial \xi^2}=\frac{e}{m_{dn}n_{d0}}\left(n_{dn0}N_{dn}+n_{dc0}N_{dc}-n_{d0}N_{d0}\right), \quad (21)$$

and

$$\frac{\partial Q_d}{\partial \tau}+M_{dc}\frac{\partial Q_d}{\partial \xi}=\frac{e}{q_{d0}}\left(\frac{n_{e0}}{n_{d0}}\right)$$
$$\times F_{ed}\left[\left\{N_e-\left(\frac{n_{i0}}{n_{e0}}\right)\left(\frac{F_{id}}{F_{ed}}\right)N_i\right\}\right.$$
$$\left.-\left(1+\frac{n_{i0}}{n_{e0}}\frac{F_{id}}{F_{ed}}\right)\right]. \quad (22)$$

Here, the independent variables like position (ξ) and time (τ) are normalized by the Jeans length (λ_J) and Jeans time (ω_J^{-1}) scales, respectively. The parameters $M_e\,(\xi)$, $M_i\,(\xi)$, $M_{dn}\,(\xi)$, and $M_{dc}\,(\xi)$ represent the flow velocities of the electrons, ions, neutral grains and charged grains normalized by the dust sound phase speed C_{ss} each. Moreover, N_e, N_i, N_{dn} and N_{dc} are the population densities of the electrons, ions, neutral grains and charged grains normalized by their equilibrium densities n_{e0}, n_{i0}, n_{dn0}, and n_{dc0}, respectively. Both the electrostatic potential Φ and self-gravitational potential Ψ are normalized by the same electron thermal potential T_p/e so as to compare their fluctuation levels on a common equivalent reference footing. The grain charge Q_d is normalized by the equilibrium grain charge q_{d0}. Lastly, the symbols F_{edc}, F_{ed}, F_{idc}, F_{id}, F_{nc} and F_{cn} are the collision frequencies of the electrons and charged grains; electrons and dust grains; ions and charged grains; ions and dust grains; neutral and charged grains; and finally, charged and neutral grains; respectively, each normalized by the Jeans frequency ω_J for our low frequency fluctuation analyses on the astrophysical scale. It may be noted that the self-gravitating large-scale plasmas are known to be inhomogeneous in nature, and so the equilibrium parameter values keep on changing from point to point [5–12,32]. Thus, adopting constant normalization parameter values dependent on the plasma variables throughout in the entire cloud is not so justifiable in such realistic situations [12]. But within the framework of the Jeans assumption of self-gravitating homogeneous medium validating local analyses [32], our choice of normalization constants dependent of the equilibrium is well justified in idealization.

We apply the standard methodology of multiple scaling techniques [6,14,16] over equations (12)–(22) to study the fluctuations within the small amplitude approximation (weak nonlinearity). Thus, the independent variables with all the usual notations are stretched into a new space defined by the coordinate transformations $X=\epsilon^{1/2}\left(\xi-\mu\tau\right)$ and $T=\epsilon^{3/2}\tau$. In the new space, the differential operators get transformed as $\partial/\partial\xi=\epsilon^{1/2}\partial/\partial X$, and $\partial^2/\partial\xi^2=\epsilon\partial^2/\partial X^2$, where μ is the phase velocity of the fluctuations (normalized by C_{ss}), and ϵ is a minor parameter characterizing the strength of nonlinearity and dispersion. Let us assume that the perturbations of our interest are local, and their wavelengths are much smaller compared to the relevant inhomogeneity scale lengths. Accordingly, the relevant dependent variables appearing in equations (12)–(22) are now expanded nonlinearly (in various ϵ-powers) around the respective equilibrium values defined under weak nonlinearity approximation (up to

the 3rd order) as follows:

$$\begin{pmatrix} N_e \\ N_i \\ N_{dn} \\ N_{dc} \\ M_e \\ M_i \\ M_{dn} \\ M_{dc} \\ \Phi \\ \Psi \\ Q_d \end{pmatrix} = \begin{pmatrix} 1 \\ 1 \\ 1 \\ 1 \\ 0 \\ 0 \\ 0 \\ 0 \\ 0 \\ 0 \\ 0 \end{pmatrix} + \epsilon \begin{pmatrix} N_{e1} \\ N_{i1} \\ N_{dn1} \\ N_{dc1} \\ M_{e1} \\ M_{i1} \\ M_{dn1} \\ M_{dc1} \\ \Phi_1 \\ \Psi_1 \\ Q_{d1} \end{pmatrix} + \epsilon^2 \begin{pmatrix} N_{e2} \\ N_{i2} \\ N_{dn2} \\ N_{dc2} \\ M_{e2} \\ M_{i2} \\ M_{dn2} \\ M_{dc2} \\ \Phi_2 \\ \Psi_2 \\ Q_{d2} \end{pmatrix} + \vdots \quad (23)$$

We now use the nonlinear expansion (23) in equations (12)–(22) for full order-by-order analyses. It is worth mentioning that there are terms involving both integral and half-integral powers on the ordering parameter ϵ. But, due to weak nonlinearity approximation [8,9,16], only the lowest-order fluctuations are considered ignoring the higher-order ones. Now, equating the like terms in various powers of ϵ from equation (12), one gets

$$\epsilon^{3/2} : \frac{\partial M_{e1}}{\partial X} - \mu \frac{\partial N_{e1}}{\partial X} = 0, \quad (24)$$

$$\epsilon^{5/2} : \frac{\partial N_{e1}}{\partial T} - \mu \frac{\partial N_{e2}}{\partial X} + N_{e1} \frac{\partial M_{e1}}{\partial X} + \frac{\partial M_{e2}}{\partial X} + M_{e1} \frac{\partial N_{e1}}{\partial X} = 0, \quad (25)$$

$$\epsilon^{7/2} : \frac{\partial N_{e2}}{\partial T} + N_{e2} \frac{\partial M_{e1}}{\partial X} + N_{e1} \frac{\partial M_{e2}}{\partial X} + M_{e2} \frac{\partial N_{e1}}{\partial X} + M_{e1} \frac{\partial N_{e2}}{\partial X} = 0, \quad (26)$$

$$\epsilon^{9/2} : N_{e2} \frac{\partial M_{e2}}{\partial X} + M_{e2} \frac{\partial N_{e2}}{\partial X} = 0, \quad (27)$$

and so on.

Again, the order-by-order analysis in various powers of ϵ from equation (13) yields

$$\epsilon^1 : \left(\frac{m_e}{m_d}\right) F_{edc} M_{e1} = 0, \quad (28)$$

$$\epsilon^2 : \left(\frac{m_e}{m_d}\right) F_{edc} \left(M_{e1} N_{e1} + M_{e2}\right) = 0, \quad (29)$$

$$\epsilon^3 : \left(\frac{m_e}{m_d}\right) F_{edc} \left(M_{e1} N_{e2} + N_{e1} M_{e2}\right) = 0, \quad (30)$$

$$\epsilon^4 : \left(\frac{m_e}{m_d}\right) F_{edc} N_{e2} M_{e2} = 0, \quad (31)$$

$$\epsilon^{3/2} : \frac{\partial N_{e1}}{\partial X} + \frac{\partial \Phi_1}{\partial X} = 0, \quad (32)$$

$$\epsilon^{5/2} : \frac{\partial N_{e2}}{\partial X} + N_{e1} \frac{\partial \Phi_1}{\partial X} + \frac{\partial \Phi_2}{\partial X} = 0, \quad (33)$$

$$\epsilon^{7/2} : N_{e2} \frac{\partial \Phi_1}{\partial X} + N_{e1} \frac{\partial \Phi_2}{\partial X} = 0, \quad (34)$$

$$\epsilon^{9/2} : N_{e2} \frac{\partial \Phi_2}{\partial X} = 0, \quad (35)$$

and so on.

This is clear that equations (28)–(31) are applicable only for $m_e/m_d \to 0$, which is $\sim 10^{-19}$ (~ 0) in our model description. In addition, higher-order harmonics have negligible variations with distance under the weak nonlinearity approximation [8,9,16], which are being neglected subsequently. Similarly, order-by-order analysis of equation (14) gives

$$\epsilon^{3/2} : \frac{\partial M_{i1}}{\partial X} - \mu \frac{\partial N_{i1}}{\partial X} = 0, \quad (36)$$

$$\epsilon^{5/2} : \frac{\partial N_{i1}}{\partial T} - \mu \frac{\partial N_{i2}}{\partial X} + N_{i1} \frac{\partial M_{i1}}{\partial X} + \frac{\partial M_{i2}}{\partial X} + M_{i1} \frac{\partial N_{i1}}{\partial X} = 0, \quad (37)$$

$$\epsilon^{7/2} : \frac{\partial N_{i2}}{\partial T} + N_{i2} \frac{\partial M_{i1}}{\partial X} + N_{i1} \frac{\partial M_{i2}}{\partial X} + M_{i2} \frac{\partial N_{i1}}{\partial X} + M_{i1} \frac{\partial N_{i2}}{\partial X} = 0, \quad (38)$$

$$\epsilon^{9/2} : N_{i2} \frac{\partial M_{i2}}{\partial X} + M_{i2} \frac{\partial N_{i2}}{\partial X} = 0, \quad (39)$$

and so forth.

The order-by-order analysis in various powers of ϵ from equation (15), similarly, yields

$$\epsilon^1 : \left(\frac{m_i}{m_d}\right) F_{idc} M_{i1} = 0, \quad (40)$$

$$\epsilon^2 : \left(\frac{m_i}{m_d}\right) F_{idc} \left(M_{i1} N_{i1} + M_{i2}\right) = 0, \quad (41)$$

$$\epsilon^3 : \left(\frac{m_i}{m_d}\right) F_{idc} \left(M_{i1} N_{i2} + N_{i1} M_{i2}\right) = 0, \quad (42)$$

$$\epsilon^4 : \left(\frac{m_i}{m_d}\right) F_{idc} N_{i2} M_{i2} = 0, \quad (43)$$

$$\epsilon^{3/2} : \frac{\partial N_{i1}}{\partial X} + \frac{\partial \Phi_1}{\partial X} = 0, \quad (44)$$

$$\epsilon^{5/2} : \frac{\partial N_{i2}}{\partial X} + N_{i1} \frac{\partial \Phi_1}{\partial X} + \frac{\partial \Phi_2}{\partial X} = 0, \quad (45)$$

$$\epsilon^{7/2} : N_{i2} \frac{\partial \Phi_1}{\partial X} + N_{i1} \frac{\partial \Phi_2}{\partial X} = 0, \quad (46)$$

$$\epsilon^{9/2} : N_{i2} \frac{\partial \Phi_2}{\partial X} = 0, \quad (47)$$

and so on.

This is seen that equations (40)–(43) are valid only for $m_i/m_d \to 0$, which is $\sim 10^{-15}$ (~ 0) in our case. Likewise, equating the terms in various powers of ϵ from both sides

of equation (16), one gets

$$\epsilon^{3/2}: \frac{\partial M_{dn1}}{\partial X} - \mu\frac{\partial N_{dn1}}{\partial X} = 0, \tag{48}$$

$$\epsilon^{5/2}: \frac{\partial N_{dn1}}{\partial T} - \mu\frac{\partial N_{dn2}}{\partial X} + N_{dn1}\frac{\partial M_{dn1}}{\partial X} + \frac{\partial M_{dn2}}{\partial X} + M_{dn1}\frac{\partial N_{dn1}}{\partial X} = 0, \tag{49}$$

$$\epsilon^{7/2}: \frac{\partial N_{dn2}}{\partial T} + N_{dn2}\frac{\partial M_{dn1}}{\partial X} + N_{dn1}\frac{\partial M_{dn2}}{\partial X} + M_{dn2}\frac{\partial N_{dn1}}{\partial X} + M_{dn1}\frac{\partial N_{dn2}}{\partial X} = 0, \tag{50}$$

$$\epsilon^{9/2}: N_{dn2}\frac{\partial M_{dn2}}{\partial X} + M_{dn2}\frac{\partial N_{dn2}}{\partial X} = 0, \tag{51}$$

and so forth.

Similar treatment on equation (17) gives,

$$\epsilon^{1}: F_{nc}\,(M_{dn1} - M_{dc1}) = 0, \tag{52}$$

$$\epsilon^{2}: F_{nc}\,(M_{dn2} - M_{dc2}) = 0, \tag{53}$$

$$\epsilon^{3/2}: \frac{1}{n_{dn0}}\frac{\partial N_{dn1}}{\partial X} - \mu\frac{\partial M_{dn1}}{\partial X} + \left(\frac{m_{dn}}{n_{dc0}e}\right)\frac{\partial \Psi_1}{\partial X} = 0, \tag{54}$$

$$\epsilon^{5/2}: \frac{\partial M_{dn1}}{\partial T} - \mu\frac{\partial M_{dn2}}{\partial X} + M_{dn1}\frac{\partial M_{dn1}}{\partial X} - \mu\, N_{dn1}\frac{\partial M_{dn1}}{\partial X} + \frac{1}{n_{dn0}}\frac{\partial N_{dn2}}{\partial X} + \left(\frac{m_{dn}}{n_{dn0}e}\right)N_{dn1}\frac{\partial \Psi_1}{\partial X} + \left(\frac{m_{dn}}{n_{dn0}e}\right)\frac{\partial \Psi_2}{\partial X} = 0, \tag{55}$$

$$\epsilon^{7/2}: \frac{\partial M_{dn2}}{\partial T} + M_{dn2}\frac{\partial M_{dn1}}{\partial X} + M_{dn1}\frac{\partial M_{dn2}}{\partial X} + N_{dn1}\frac{\partial M_{dn1}}{\partial T} - \mu\, N_{dn1}\frac{\partial M_{dn2}}{\partial X} + N_{dn1}M_{dn1}\frac{\partial M_{dn1}}{\partial X} - \mu\, N_{dn2}\frac{\partial M_{dn1}}{\partial X} + \left(\frac{m_{dn}}{n_{dn0}e}\right)N_{dn2}\frac{\partial \Psi_1}{\partial X} + \left(\frac{m_{dn}}{n_{dn0}e}\right)N_{dn1}\frac{\partial \Psi_2}{\partial X} = 0, \tag{56}$$

$$\epsilon^{9/2}: M_{dn2}\frac{\partial M_{dn2}}{\partial X} + N_{dn1}\frac{\partial M_{dn2}}{\partial T} + N_{dn1}M_{dn2}\frac{\partial M_{dn1}}{\partial X} + N_{dn1}M_{dn1}\frac{\partial M_{dn2}}{\partial X} + N_{dn2}\frac{\partial M_{dn1}}{\partial T} - \mu\, N_{dn2}\frac{\partial M_{dn2}}{\partial X} + N_{dn2}M_{dn1}\frac{\partial M_{dn1}}{\partial X} + \left(\frac{m_{dn}}{n_{dn0}e}\right)N_{dn2}\frac{\partial \Psi_2}{\partial X} = 0, \tag{57}$$

$$\epsilon^{11/2}: N_{dn1}M_{dn2}\frac{\partial M_{dn2}}{\partial X} + N_{dn2}\frac{\partial M_{dn1}}{\partial T} + N_{dn2}M_{dn2}\frac{\partial M_{dn1}}{\partial X} + N_{dn2}M_{dn1}\frac{\partial M_{dn2}}{\partial X} = 0, \tag{58}$$

$$\epsilon^{14/2}: N_{dn2}M_{dn2}\frac{\partial M_{dn2}}{\partial X} = 0, \quad \text{and so on.} \tag{59}$$

One can see from equations (52)–(53) that the velocity perturbations of the neutral and charged grains are equal due obviously to the consideration of identical spherical grains each with mass m_d. Again, equating the like terms from both sides of equation (18), one gets

$$\epsilon^{3/2}: \frac{\partial M_{dc1}}{\partial X} - \mu\frac{\partial N_{dc1}}{\partial X} = 0, \tag{60}$$

$$\epsilon^{5/2}: \frac{\partial N_{dc1}}{\partial T} - \mu\frac{\partial N_{dc2}}{\partial X} + N_{dc1}\frac{\partial M_{dc1}}{\partial X} + \frac{\partial M_{dc2}}{\partial X} + M_{dc1}\frac{\partial N_{dc1}}{\partial X} = 0, \tag{61}$$

$$\epsilon^{7/2}: \frac{\partial N_{dc2}}{\partial T} + N_{dc2}\frac{\partial M_{dc1}}{\partial X} + N_{dc1}\frac{\partial M_{dc2}}{\partial X} + M_{dc2}\frac{\partial N_{dc1}}{\partial X} + M_{dc1}\frac{\partial N_{dc2}}{\partial X} = 0, \tag{62}$$

$$\epsilon^{9/2}: N_{dc2}\frac{\partial M_{dc2}}{\partial X} + M_{dc2}\frac{\partial N_{dc2}}{\partial X} = 0, \tag{63}$$

and so on.

The order-by-order analysis in various powers of ϵ from equation (19) yields

$$\epsilon^{1}: F_{cn}\,(M_{dc1} - M_{dn1}) = 0, \tag{64}$$

$$\epsilon^{2}: F_{cn}\,(M_{dc2} - M_{dn2}) = 0, \tag{65}$$

$$\epsilon^{3/2}: \frac{1}{n_{dc0}}\frac{\partial N_{dc1}}{\partial X} - \mu\frac{\partial M_{dc1}}{\partial X} + \left(\frac{m_{dc}}{n_{dc0}e}\right)\frac{\partial \Psi_1}{\partial X} = 0, \tag{66}$$

$$\epsilon^{5/2}: \frac{\partial M_{dc1}}{\partial T} - \mu\frac{\partial M_{dc2}}{\partial X} + M_{dc1}\frac{\partial M_{dc1}}{\partial X} - \mu\, N_{dc1}\frac{\partial M_{dc1}}{\partial X} + \frac{1}{n_{dc0}}\frac{\partial N_{dc2}}{\partial X} + \left(\frac{m_{dc}}{n_{dc0}e}\right)N_{dc1}\frac{\partial \Psi_1}{\partial X} + \left(\frac{m_{dc}}{n_{dc0}e}\right)\frac{\partial \Psi_2}{\partial X} + \left(\frac{q_{d0}}{n_{dc0}}\right)Q_{d1}\frac{\partial \Phi_1}{\partial X} = 0, \tag{67}$$

$$\epsilon^{7/2}: \frac{\partial M_{dc2}}{\partial T} + M_{dc2}\frac{\partial M_{dc1}}{\partial X} + M_{dc1}\frac{\partial M_{dc2}}{\partial X} + N_{dc1}\frac{\partial M_{dc1}}{\partial T} - \mu\, N_{dc1}\frac{\partial M_{dc2}}{\partial X} + N_{dc1}M_{dc1}\frac{\partial M_{dc1}}{\partial X} - \mu\, N_{dc2}\frac{\partial M_{dc1}}{\partial X} + \left(\frac{m_{dc}}{n_{dc0}e}\right)N_{dc2}\frac{\partial \Psi_1}{\partial X} + \left(\frac{m_{dc}}{n_{dc0}e}\right)N_{dc1}\frac{\partial \Psi_2}{\partial X} + \left(\frac{q_{d0}}{n_{dc0}}\right)Q_{d2}\frac{\partial \Phi_1}{\partial X} + \left(\frac{q_{d0}}{n_{dc0}}\right)Q_{d1}N_{dc1}\frac{\partial \Phi_1}{\partial X} + \left(\frac{q_{d0}}{n_{dc0}}\right)Q_{d1}\frac{\partial \Phi_2}{\partial X} = 0, \tag{68}$$

$$\epsilon^{9/2}: M_{dc2}\frac{\partial M_{dc2}}{\partial X}+N_{dc1}\frac{\partial M_{dc2}}{\partial T}+N_{dc1}M_{dc2}\frac{\partial M_{dc1}}{\partial X}+N_{dc1}M_{dc1}\frac{\partial M_{dc2}}{\partial X}+N_{dc2}\frac{\partial M_{dc1}}{\partial T}-\mu\,N_{dc2}\frac{\partial M_{dc2}}{\partial X}+N_{dc2}M_{dc1}\frac{\partial M_{dc1}}{\partial X}+\left(\frac{m_{dc}}{n_{dc0}e}\right)N_{dc2}\frac{\partial \Psi_2}{\partial X}+\left(\frac{q_{d0}}{n_{dc0}}\right)Q_{d2}N_{dc1}\frac{\partial \Phi_1}{\partial X}+\left(\frac{q_{d0}}{n_{dc0}}\right)Q_{d1}N_{dc2}\frac{\partial \Phi_1}{\partial X}+\left(\frac{q_{d0}}{n_{dc0}}\right)Q_{d2}\frac{\partial \Phi_2}{\partial X}+\left(\frac{q_{d0}}{n_{dc0}}\right)Q_{d1}N_{dc1}\frac{\partial \Phi_2}{\partial X}=0, \tag{69}$$

$$\epsilon^{11/2}: N_{dc1}M_{dc2}\frac{\partial M_{dc2}}{\partial X}+N_{dc2}\frac{\partial M_{dc1}}{\partial T}+N_{dc2}M_{dc2}\frac{\partial M_{dc1}}{\partial X}+N_{dc2}M_{dc1}\frac{\partial M_{dc2}}{\partial X}+\left(\frac{q_{d0}}{n_{dc0}}\right)Q_{d2}N_{dc2}\frac{\partial \Phi_1}{\partial X}+\left(\frac{q_{d0}}{n_{dc0}}\right)Q_{d2}N_{dc1}\frac{\partial \Phi_2}{\partial X}+\left(\frac{q_{d0}}{n_{dc0}}\right)Q_{d1}N_{dc2}\frac{\partial \Phi_2}{\partial X}=0, \tag{70}$$

$$\epsilon^{14/2}: N_{dc2}M_{dc2}\frac{\partial M_{dc2}}{\partial X}+\left(\frac{q_{d0}}{n_{dc0}}\right)Q_{d2}N_{dc2}\frac{\partial \Phi_2}{\partial X}=0, \tag{71}$$

and so on.

We see that here too, the implications of equations (64) and (65) are the same as in the case of equations (52)–(53). The order-by-order analysis in various powers of ϵ from equation (20), similarly, yields

$$\epsilon^0: \frac{e^2}{m_{dc}^2 n_{d0} G}\left(n_{e0}-n_{i0}\right)=0, \tag{72}$$

$$\epsilon^1: \frac{e}{m_{dc}^2 n_{d0} G}\left(e n_{e0}N_{e1}-e n_{i0}N_{i1}+q_{d0}n_{dc0}Q_{d1}\right)=0, \tag{73}$$

$$\epsilon^2: \frac{\partial^2 \Phi_1}{\partial X^2}=\frac{e}{m_{dc}^2 n_{d0} G}\left(e n_{e0}N_{e2}-e n_{i0}N_{i2}+q_{d0}n_{dc0}Q_{d2}+q_{d0}n_{dc0}Q_{d1}N_{dc1}\right), \tag{74}$$

$$\epsilon^3: \frac{\partial^2 \Phi_2}{\partial X^2}=\frac{e}{m_{dc}^2 n_{d0} G}\times\left(q_{d0}n_{dc0}Q_{d2}N_{dc1}+q_{d0}n_{dc0}Q_{d1}N_{dc2}\right), \tag{75}$$

$$\epsilon^4: q_{d0}n_{dc0}Q_{d2}N_{dc2}=0, \tag{76}$$

and so on.

From equation (21), similarly, order-by-order analysis yields

$$\epsilon^0: \frac{e}{m_{dn}n_{d0}}\left(n_{dn0}+n_{dc0}-n_{d0}\right)=0, \tag{77}$$

$$\epsilon^1: \frac{e}{m_{dn}n_{d0}}\left(n_{dn0}N_{dn1}+n_{dc0}N_{dc1}\right)=0, \tag{78}$$

$$\epsilon^2: \frac{\partial^2 \Psi_1}{\partial X^2}=\frac{e}{m_{dn}n_{d0}}\left(n_{dn0}N_{dn2}+n_{dc0}N_{dc2}\right), \tag{79}$$

$$\epsilon^3: \frac{\partial^2 \Psi_2}{\partial X^2}=0, \tag{80}$$

and so on.

Lastly, equating the terms in various powers of ϵ from equation (22), one gets

$$\epsilon^0: -\frac{2e\,n_{i0}}{q_{d0}n_{d0}}F_{id}=0, \tag{81}$$

$$\epsilon^1: \frac{e}{q_{d0}}\left(\frac{n_{e0}}{n_{d0}}\right)F_{ed}\left\{N_{e1}-\left(\frac{n_{i0}}{n_{e0}}\right)\frac{F_{id}}{F_{ed}}N_{i1}\right\}=0, \tag{82}$$

$$\epsilon^2: \frac{e}{q_{d0}}\left(\frac{n_{e0}}{n_{d0}}\right)F_{ed}\left\{N_{e2}-\left(\frac{n_{i0}}{n_{e0}}\right)\frac{F_{id}}{F_{ed}}N_{i2}\right\}=0, \tag{83}$$

$$\epsilon^{3/2}: -\mu\frac{\partial Q_{d1}}{\partial X}=0, \tag{84}$$

$$\epsilon^{5/2}: \frac{\partial Q_{d1}}{\partial T}-\mu\frac{\partial Q_{d2}}{\partial X}+M_{dc1}\frac{\partial Q_{d1}}{\partial X}=0, \tag{85}$$

$$\epsilon^{7/2}: \frac{\partial Q_{d2}}{\partial T}+M_{dc2}\frac{\partial Q_{d1}}{\partial X}+M_{dc1}\frac{\partial Q_{d1}}{\partial X}=0, \tag{86}$$

$$\epsilon^{9/2}: M_{dc2}\frac{\partial Q_{d2}}{\partial X}=0, \tag{87}$$

and so forth.

It may be noticed that equation (81) is applicable for very strongly charged dust grains so that the reciprocal of their equilibrium charge, $1/q_{d0}\to 0$. Our underlying approximation of weak nonlinearity is justifiably reflected in all equations (24)–(87), where higher-order harmonics get self-consistently negligible due normally to weak nonlinearity in the simplified proposed model. Now, after simplifying equation (74), by eliminating the second-order perturbed quantities using the various relations within equations (24)–(73) and (75)–(87), we get the following d-KdV equation describing the nonlinear electrostatic fluctuations (in terms of Φ_1), expressed as:

$$\frac{\partial \Phi_1}{\partial T}+A_1\Phi_1\frac{\partial \Phi_1}{\partial X}+B_1\frac{\partial^3 \Phi_1}{\partial X^3}=C_1\Phi_1^2\frac{\partial \Phi_1}{\partial X}, \tag{88}$$

where, the response coefficients A_1 (convective), B_1 (dispersive) and C_1 (driving), dependent on the equilibrium cloud parameters, are defined by:

$$A_1=-\mu,\quad B_1=\frac{m_{dc}^2 n_{d0}G\mu}{e^2\left(n_{e0}-n_{i0}\right)},\quad C_1=-\frac{\left(e n_{e0}-e n_{i0}\right)}{n_{dc0}^2\mu}. \tag{89}$$

Thus, the electrostatic eigenmodes are collectively governed by equation (88) having a self-consistent nonlinear source term. The effect of grain-mass appears in B_1, and so, the third term in equation (88) represents the grain inertial outcome on the fluctuation dynamics.

Again, by simplifying equation (79), with elimination procedure of the second-order perturbed quantities using the various relations within equations (24)–(78) and (80)–(87), we obtain the following KdV equation depicting the nonlinear self-gravitational fluctuations (in terms of Ψ_1), which is presented as:

$$\frac{\partial \Psi_1}{\partial T}+A_2\Psi_1\frac{\partial \Psi_1}{\partial X}+B_2\frac{\partial^3 \Psi_1}{\partial X^3}=0, \tag{90}$$

where, the response coefficients A_2 (convective) and B_2 (dispersive), dependent on the diverse DMC parameters,

are given by:

$$A_2 = \frac{\mu\, m_{dn}\left(1 - n_{dn0}\mu^2\right)^2}{e\left(n_{ndo}\mu^2 - 1\right)^3} + \frac{1}{2en_{dn0}\mu},$$
$$B_2 = \frac{n_{d0}\left(1 - n_{dn0}\mu^2\right)^2}{2\mu\, n_{dn0}^2}. \quad (91)$$

As a result, the self-gravitational fluctuations are collectively governed by equation (90) having no self-consistent source term, as in contrast with the case of electrostatic counterpart. The effect of grain-mass appears in A_2, and consequently, the first term in equation (90) represents the grain inertial effect on the associated fluctuation dynamics.

The basic characteristics of the fluctuation dynamics, and associated evolutionary eigenmode structures can conveniently be studied with the help of time-stationary (steady-state) solutions [8,9,16]. Thus, for computational simplicity, equations (88) and (90) are transformed into ordinary differential equations (ODEs) by the Galilean type (commoving) of coordinate transformation $\rho = X - T$ so that $\partial/\partial X = \partial/\partial\rho$ and $\partial/\partial T = -\partial/\partial\rho$ without any loss of generality of the considered fluctuation dynamics as follows:

$$\frac{\partial\Phi_1}{\partial\rho} - A_1\Phi_1\frac{\partial\Phi_1}{\partial\rho} - B_1\frac{\partial^3\Phi_1}{\partial\rho^3} = -C_1\Phi_1^2\frac{\partial\Phi_1}{\partial\rho}, \quad (92)$$

and

$$\frac{\partial\Psi_1}{\partial\rho} - A_2\Psi_1\frac{\partial\Psi_1}{\partial\rho} - B_2\frac{\partial^3\Psi_1}{\partial\rho^3} = 0. \quad (93)$$

The explicit analytical solutions of equations (92) and (93) in the asymptotically zero limit of the fluctuations, and their gradients as a solitonic spectrum are well-known [16]. For observing exact microphysical details of the eigenmodes patterns, numerical techniques are being adopted.

5 Numerical calculation scheme

The collective KdV system obtained analytically is numerically integrated as initial value problems, by adopting the fourth-order Runge-Kutta method, to pictorialize the basic microphysical features of the lowest-order diverse electro-gravitational fluctuation dynamics in response to a sensible multi-parameter variation. The numerically obtained profiles of the steady-state structures of the electrostatic eigenmode spectral patterns and related properties of the cloud (after Eq. (92)) are graphically displayed in Figures 1–3. Figure 1 depicts the profile structures of the lowest-order perturbed electrostatic (a) potential (Φ_1), (b) field ($-\Phi_{1\rho}$), (c) potential curvature ($\Phi_{1\rho\rho}$), and (d) phase portrait (in phase space defined by Φ_1 and $\Phi_{1\rho}$). Various lines correspond to case (1): $m_d = 2.08 \times 10^{-12}$ kg (blue line), case (2): $m_d = 4.14 \times 10^{-12}$ kg (red line), case (3): $m_d = 6.21 \times 10^{-12}$ kg (green line), and case (4): $m_d = 8.28 \times 10^{-12}$ kg (black line), respectively. Different input initial values used are $(\Phi)_i = 1.00 \times 10^{-7}$, $(\Phi_\rho)_i = -2.00 \times 10^{-7}$, and $(\Phi_{\rho\rho})_i = 1.00 \times 10^{-3}$. The other parameters kept fixed are $n_{e0} = 2.01 \times 10^{12}$ m^{-3}, $n_{i0} = 4.95 \times 10^{12}$ m^{-3}, $n_{dn0} = 4.20 \times 10^6$ m^{-3}, $n_{dc0} = 2.35 \times 10^6$ m^{-3} and $\mu = 1.01$. It is seen that the electrostatic fluctuations (Fig. 1a), fields (Fig. 1b) and fluctuation curvatures (Fig. 1c) evolve like solitonic spectral patterns (extended and chain) as a conservative dynamics with closed form of phase space geometry (Fig. 1d). Figure 2 shows the same as Figure 1, but with $m_d = 8.28 \times 10^{-12}$ kg. Various lines correspond to case (1): $n_{dn0} = 8.50 \times 10^6$ m^{-3} (blue line), case (2): $n_{dn0} = 1.97 \times 10^7$ m^{-3} (red line), case (3): $n_{dn0} = 3.08 \times 10^7$ m^{-3} (green line), and case (4): $n_{dn0} = 4.20 \times 10^7$ m^{-3} (black line), respectively. Lastly, Figure 3 portrays the same as Figure 1, but with $m_d = 8.28 \times 10^{-12}$ kg. Various lines correspond to case (1): $\mu = 0.25$ (blue line), case (2): $\mu = 0.50$ (red line), case (3): $\mu = 0.75$ (green line), and case (4): $\mu = 1.01$ (black line), respectively.

The graphical structures of the self-gravitational fluctuation dynamics obtained numerically (after Eq. (93)) under judicious multi-parameter variation scheme to examine the detailed features of the eigenmode formation are displayed in Figures 4 and 5. Figure 4 shows the profiles of the lowest-order perturbed self-gravitational (a) potential (Ψ_1), (b) field ($-\Psi_{1\rho}$), (c) potential curvature ($\Psi_{1\rho\rho}$), and (d) phase portrait (in phase space defined by Ψ_1 and $\Psi_{1\rho}$). Various lines correspond to case (1): $n_{dn0} = 5.90 \times 10^7$ m^{-3} (blue line), case (2): $n_{dn0} = 1.20 \times 10^8$ m^{-3} (red line), case (3): $n_{dn0} = 1.81 \times 10^8$ m^{-3} (green line), and case (4): $n_{dn0} = 2.42 \times 10^8$ m^{-3} (black line), respectively. Different input initial values used are $(\Psi)_i = 1.00 \times 10^{-7}$, $(\Psi_\rho)_i = -2.00 \times 10^{-7}$, and $(\Psi_{\rho\rho})_i = 1.00 \times 10^{-3}$. The other parameters kept fixed are $\mu = 0.96$, $n_{dn0} = 2.42 \times 10^8$ m^{-3}, $n_{dc0} = 6.43 \times 10^6$ m^{-3} and $m_d = 8.28 \times 10^{-12}$. Lastly, Figure 5 presents the same as Figure 4. Various lines correspond to case (1): $\mu = 0.32$ (blue line), case (2): $\mu = 0.53$ (red line), case (3): $\mu = 0.74$ (green line), and case (4): $\mu = 0.96$ (black line), respectively.

6 Results and discussions

This work focuses on the development of a simplified calculation scheme to show the nature of the nonlinear gravito-electrostatic fluctuation dynamics in DMC in the small-amplitude limit (weak nonlinearity). We use the well-known Jeans assumption of uniform self-gravitating homogeneous medium in normalizing our simplified model setup. It is seen that the eigenmode evolutions on the Jeans scale are expressible by a new KdV system derived by multiple scaling technique. Numerical simulation shows that both the classes (electrostatic and self-gravitational) of eigenmodes undergo a unique transition of soliton-chain to single soliton-type eigenmodes (Figs. 1a–5a) in some judiciously chosen diverse plasma conditions. The associated field fluctuations evolve as periodic waves (Figs. 1b–5b). The electrostatic instabilities introduce the corresponding fluctuations in the perturbed plasma quasi-neutrality conditions (Figs. 1c–3c) as well, where $(0, 0, 0)$ for $(\rho, \Phi_1, \Phi_{1\rho})$

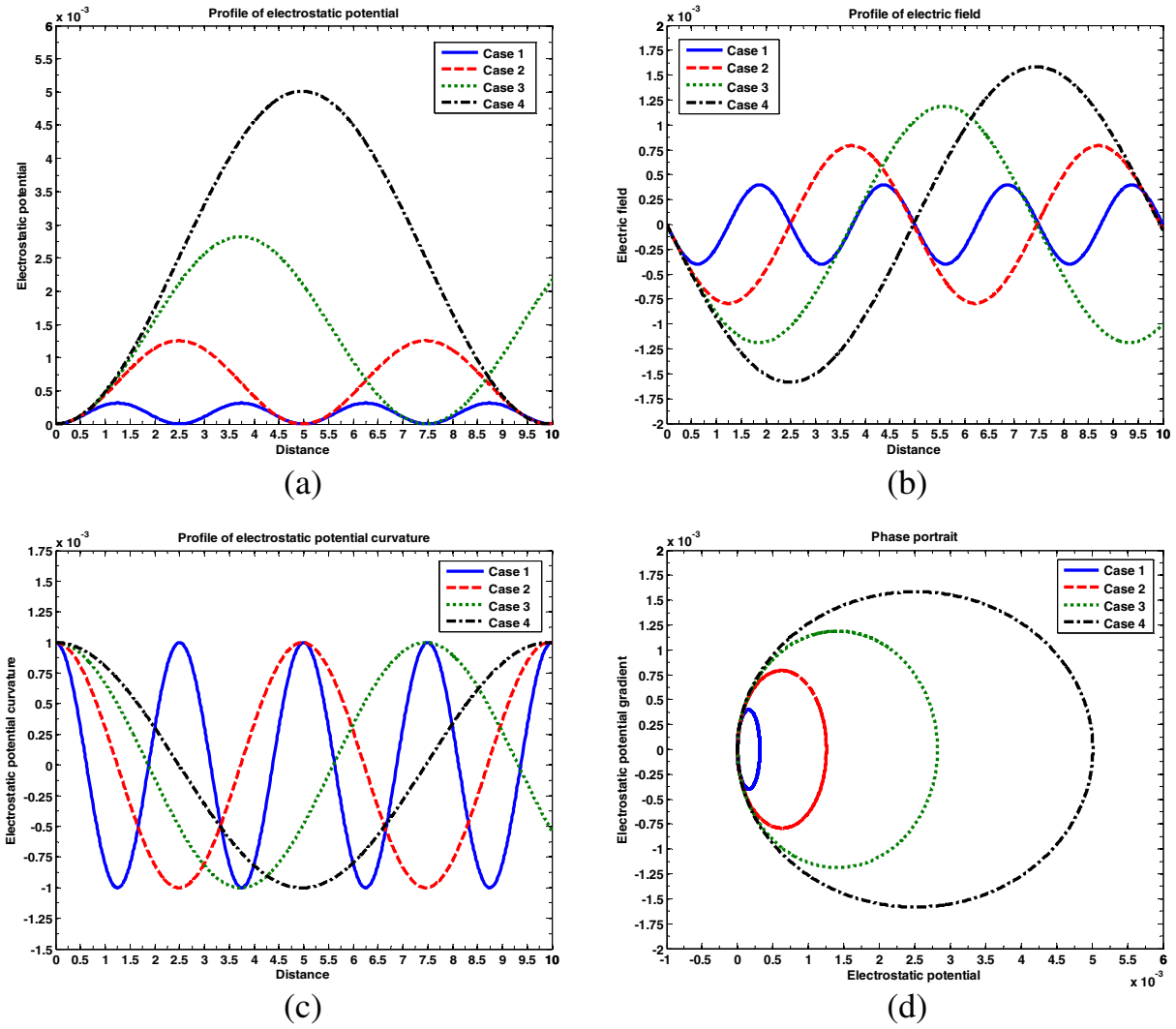

Fig. 1. Profile of the lowest-order perturbed electrostatic (a) potential, (b) field, (c) potential curvature, and (d) phase portrait. Various lines correspond to case (1): $m_d = 2.08 \times 10^{-12}$ kg (blue line), case (2): $m_d = 4.14 \times 10^{-12}$ kg (red line), case (3): $m_d = 6.21 \times 10^{-12}$ kg (green line), and case (4): $m_d = 8.28 \times 10^{-12}$ kg (black line), respectively. Different input initial values used are $(\Phi)_i = 1.00 \times 10^{-7}$, $(\Phi_\rho)_i = -2.00 \times 10^{-7}$, and $(\Phi_{\rho\rho})_i = 1.00 \times 10^{-3}$. The other parameters kept fixed are, $n_{e0} = 2.01 \times 10^{12}$ m^{-3}, $n_{i0} = 4.95 \times 10^{12}$ m^{-3}, $n_{dn0} = 4.20 \times 10^{7}$ m^{-3}, $n_{dc0} = 2.53 \times 10^{6}$ m^{-3}, $\mu = 1.01$, $G = 6.67 \times 10^{-11}$ N m^2 kg^{-2}, and $e = 1.67 \times 10^{-19}$ C.

is the most stable focal point for the evolution of the fluctuations (Figs. 1d–3d).

Analogous to the electrostatic fluctuation evolutions (Figs. 1–3), the self-gravitational eigenmode dynamics too shows miscellaneous solitary spectral patterns (Figs. 4 and 5). As the equilibrium value of the neutral dust-grain density increases, the self-gravitational potential fluctuation undergoes an interesting dynamical transition from solitary chain (smaller amplitude) to a two-tail extended compressive soliton (larger amplitude), and vice versa (Fig. 4a). The corresponding field fluctuation shows a composite mixture of compressive and rarefactive solitary patterns (Fig. 4b). The associated potential curvature is a bell-shaped (rarefactive) solitary shapes (Fig. 4c). The phase space trajectories evolve as closed-form patterns showing conservative signatures of the dynamics (Fig. 4d). With variation in the reference frame velocity as well, similar self-gravitational eigenmode features are observed (Fig. 5). The self-gravitational fluctuation phase portraits too show that (0, 0, 0) for $(\rho, \Psi_1, \Psi_{1\rho})$ is the most stable focal point of the dynamical evolution of the fluctuations (Figs. 4d–5d). Our theoretical analyses allow us to summarize the following main points of space and astrophysical concerns.

1. The nonlinear gravito-electrotatic (pulsational) fluctuation dynamics in presence of variable-charge grains and all the possible collisional effects in planar geometry are collectively governed by new uncoupled pair KdV equations obtained by multiple scaling technique. The electrostatic eigenmodes are expressible by the d-KdV equation having a self-consistent nonlinear driving source. The source naturally arises due to the electron-ion ambipolar polarization effect leading

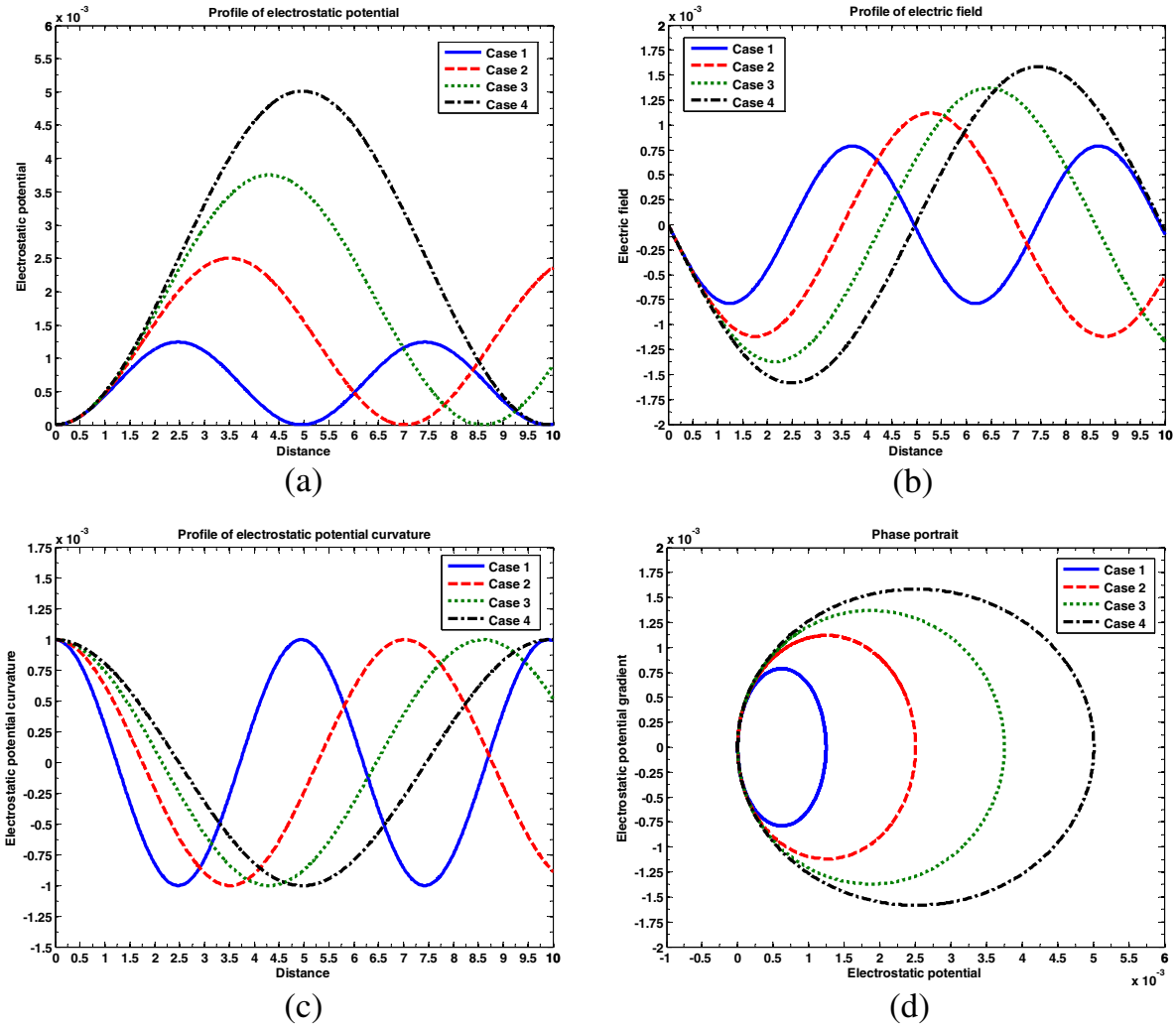

Fig. 2. Same as Figure 1, but with $m_d = 8.28 \times 10^{-12}$ kg. Various lines correspond to case (1): $n_{dn0} = 8.50 \times 10^6$ m^{-3} (blue line), case (2): $n_{dn0} = 1.97 \times 10^7$ m^{-3} (red line), case (3): $n_{dn0} = 3.08 \times 10^7$ m^{-3} (green line), and case (4): $n_{dn0} = 4.20 \times 10^7$ m^{-3} (black line), respectively.

to dust-charge fluctuation, equilibrium charged grain density and reference frame velocity. Although weak, the source vanishes completely for (1) $n_{e0} = n_{i0}$, (2) $\mu \to \infty$, and (3) $n_{dc0} \to \infty$ (as clearly evident from Eq. (89)). Likewise, the self-gravitational counterparts of the fluctuations are collectively describable by the KdV equation (with no source). All the fluctuations are co-excited within an integrated interplay of diverse nonlinear (hydrodynamic cause), dispersive (self-gravitational cause) and weakly dissipative (collisional cause) effects cooperatively.

2. The electrostatic fluctuations undergo a new transition from soliton-chain to single-soliton type eigenmode with increase in grain mass (Fig. 1a). This may be at the cost of self-gravitational effects, which increase with increase in grain-mass, and vice versa.
3. The amplitude of the electrostatic fluctuations increases with increase in the equilibrium neutral dust population density, and vice versa (Fig. 2a). As the equilibrium neutral dust density increases, it thereby increases the charged dust population density by collisions. Thus, the electrostatic repulsive force among the like charged grains, and hence, charge-fluctuation increase. This, in turn, enhances the magnitude of the electrostatic fluctuations.
4. It is seen that with increase in fluctuation phase speed (or, reference frame velocity), there is an interesting transition from soliton-chain to single soliton-type eigenmode (Fig. 3a), as before (Fig. 1a). The compressive solitary amplitude increases with increase in the phase speed, and vice versa.
5. The amplitude of the self-gravitational fluctuations increases with increase in equilibrium neutral dust population density, and vice versa (Fig. 4a). This is because of increase in self-gravitational attraction with increase in equilibrium neutral dust-population density.
6. Besides, as the fluctuation phase speed (or, reference frame velocity) increases, there is a transition from soliton-chain to single soliton-type eigenmode (Fig. 5a), as before (Fig. 3a). Thus, the

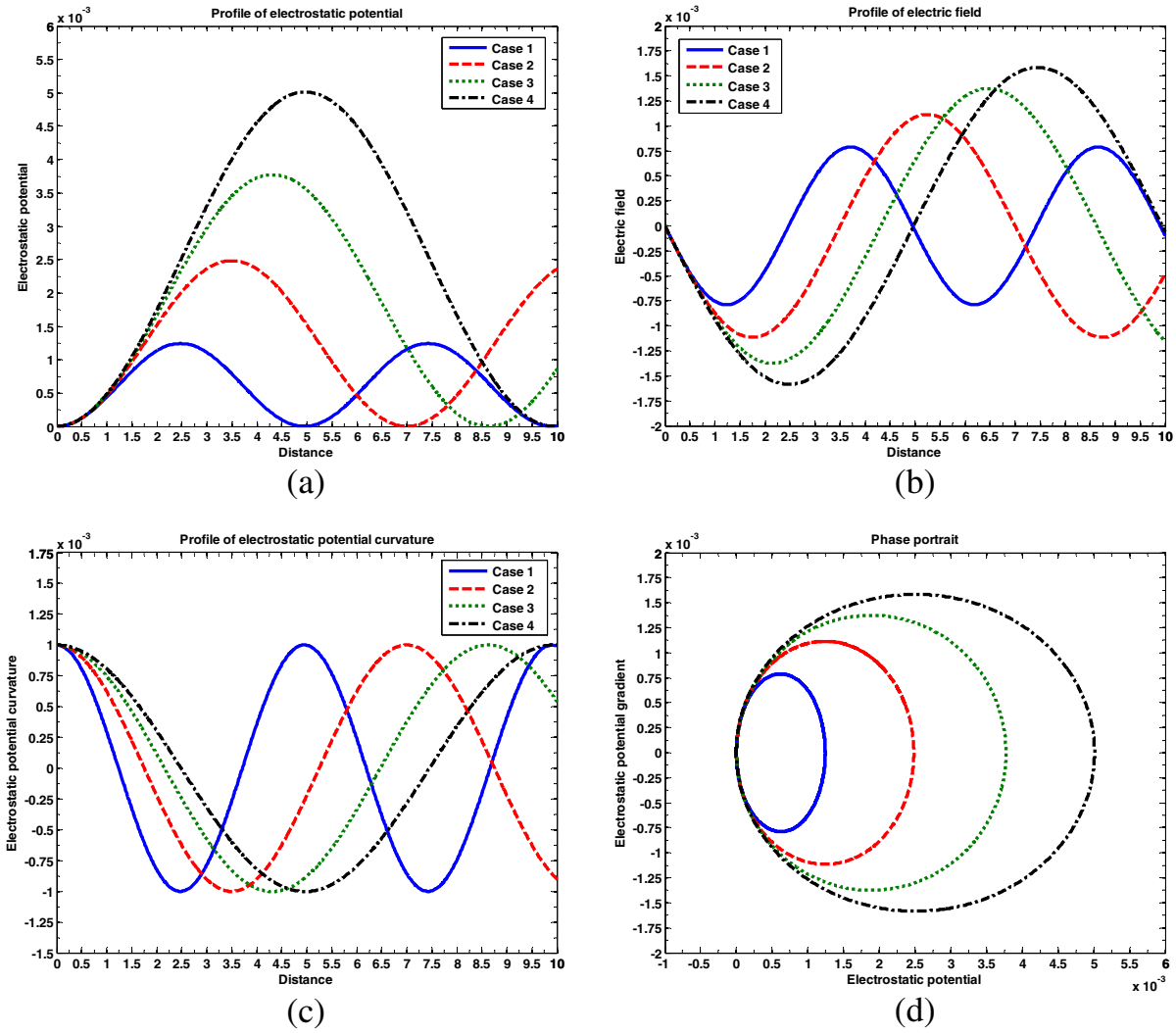

Fig. 3. Same as Figure 1, but with $m_d = 8.28 \times 10^{-12}$ kg. Various lines correspond to case (1): $\mu = 0.25$ (blue line), case (2): $\mu = 0.50$ (red line), case (3): $\mu = 0.75$ (green line), and case (4): $\mu = 1.01$ (black line), respectively.

self-gravitational fluctuation amplitude increases with the reference frame velocity, and vice versa.

7. Furthermore, the periodic nature of all the observed eigenmodes (Figs. 1a–5a), associated fields (Figs. 1b–5b), and potential curvatures (Figs. 1c–5c) is due basically to the continuous intermittent interplay of the self-gravitational attraction (inflow) and electrostatic repulsion (outflow) contributed by various constituent particles of the cloud. Moreover, the closed-form structures of the electrostatic phase portraits (Figs. 1d–3d) contributed by the Coulombic particles and self-gravitational phase portraits (Figs. 4d–5d) contributed by the Newtonian particles show that the gravito-electrostatic fluctuation dynamics evolves as a conservative dynamical (KdV) system. This may, in addition, be noted that the self-consistent nonlinear source arising in the electrostatic d-KdV equation has a strength ($\sim 10^{-20}$, estimated with all the standard values of the relevant normalized parameters [11]) too small to affect the conservative fluctuation dynamics.

8. Lastly, for quantitative comparison, let us consider the HII region for which $T_p = 10^4$ K ~ 1 eV so that $T_p/e \sim 1$ V [11], and $\epsilon \sim 10^{-2}$ [16]. From Figures 1a–3a, $\Phi_1 \sim 10^{-3}$, which is physically $\phi_{phys} \sim \epsilon\Phi_1 \sim 10^{-5}$ V. Again from Figure 4a–5a, $\Psi_1 \sim 10^{-3}$, which is physically $\psi_{phys} \sim \epsilon\Psi_1 \sim 10^{-5}$ V (on the same electrostatic equivalence units). Thus, $\phi_{phys}/\psi_{phys} \sim 1$, and so, the gravito-electrostatic fluctuation scales overlap. This illustrates that in a collapsing cloud, the grains with such characteristics may exist in the inner region of the protostellar disk, as the grain-size always increases towards the central condensation. This is in good correspondence with the earlier results valid for comparable gravito-electrostatic strengths contributed by the grains not too massive [5,6]. The grains of similar features are expected to successfully explain most of the observational dynamics of galaxies like magneto-gravitational instabilities [21] and disparate astrophysical environments [8–13,18–32].

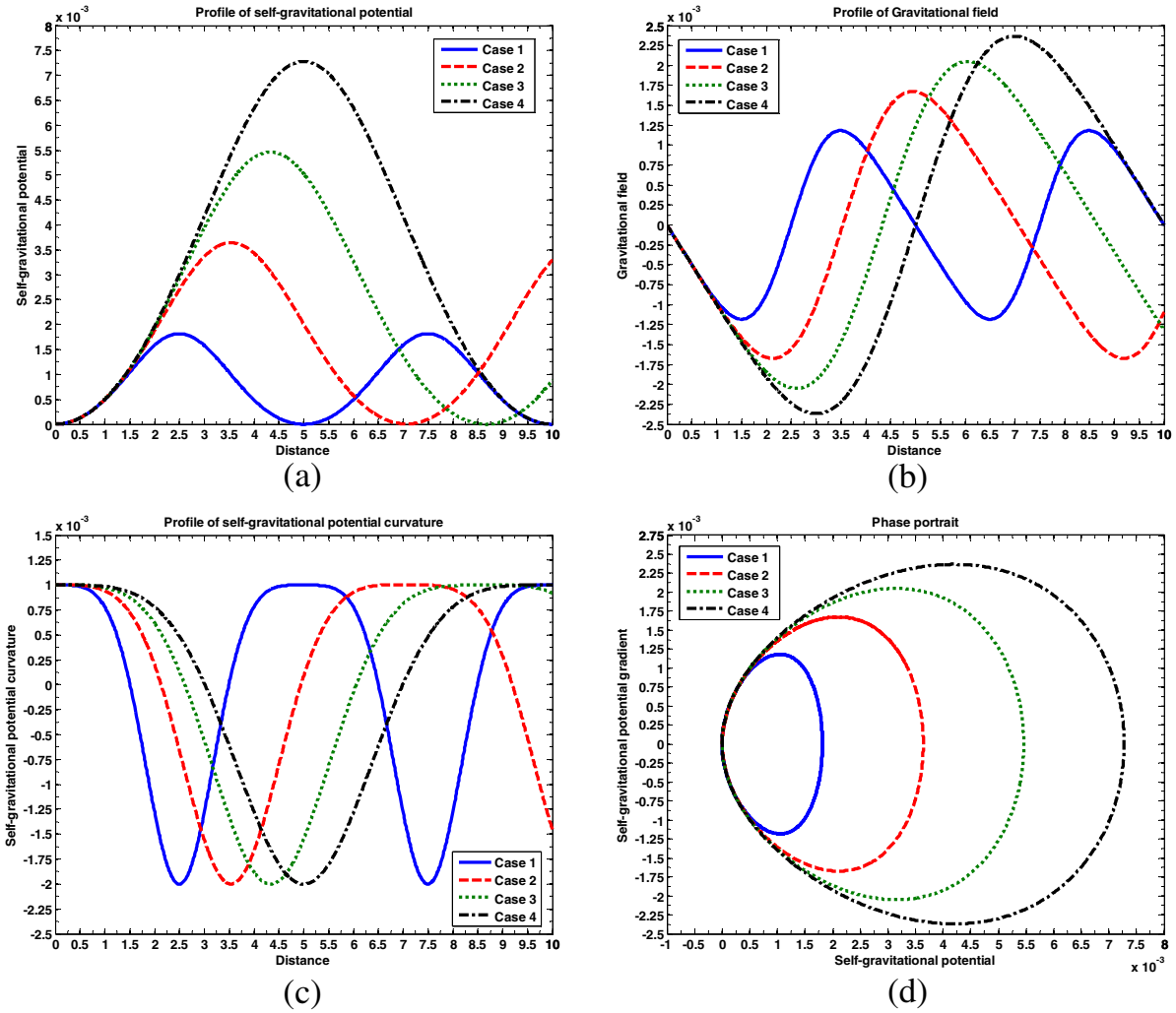

Fig. 4. Profile of the lowest-order perturbed self-gravitational (a) potential, (b) field, (c) potential curvature, and (d) phase portrait. Various lines correspond to case (1): $n_{dn0} = 5.90 \times 10^7$ m^{-3} (blue line), case (2): $n_{dn0} = 1.20 \times 10^8$ m^{-3} (red line), case (3): $n_{dn0} = 1.81 \times 10^8$ m^{-3} (green line), and case (4): $n_{dn0} = 2.42 \times 10^8$ m^{-3} (black line), respectively. Different input initial values used are $(\Psi)_i = 1.00 \times 10^{-7}$, $(\Psi_\rho)_i = -2.00 \times 10^{-7}$, and $(\Psi_{\rho\rho})_i = 1.00 \times 10^{-3}$. The other parameters kept fixed are $\mu = 0.96$, $n_{dn0} = 2.42 \times 10^8$ m^{-3}, $n_{dc0} = 6.43 \times 10^6$ m^{-3} and $m_d = 8.28 \times 10^{-12}$.

7 Conclusions

We develop a simplified theoretical evolutionary model to analyze the coexcitation of different nonlinear gravito-electrostatic eigenmodes supported in a field-free planar (1D) DMC in presence of dust-charge fluctuation, convection and collision on the astrophysical scale. First, we construct the normalized set of the basic structure equations in a coupled form using the Jeans assumption of self-gravitating homogeneous medium. Then, a standard methodology of multiple scaling technique is used over the cloud equilibrium to derive the eigenmode evolution equations. It is shown that the electrostatic eigenmodes appear in the form of solitary spectral patterns collectively governed by a unique d-KdV equation containing a self-consistent nonlinear driving source arising due to deviation from quasi-neutrality. The self-gravitational fluctuations, on the other hand, are proved to evolve like a similar solitary pattern, but dictated by a KdV equation without any source. In addition, exact numerical (by the fourth-order Runge-Kutta method) forms of the coexisting distinct classes of the eigenmodes are derived. The associated field fluctuations, perturbed potential curvatures, and phase potraits are studied with multi-parameter variation in detail. We see that the gravito-electrostatic eigenmodes evolve like a conservative system against weak fluctuations ($\leq$ the 3rd order).

Although simplified and idealized in methodologies, our proposed model calculations allow us to draw the following main conclusive remarks having new astrophysical significance.

1. The nonlinear gravito-electrostatic eigenmodes supported in a planar field-free self-gravitating DMC in quasi-neutral hydrodynamic equilibrium are collectively governed by a new pair of the KdV-type equations (electrostatic d-KdV, and self-gravitational KdV), instead of a single nonlinear evolution equation,

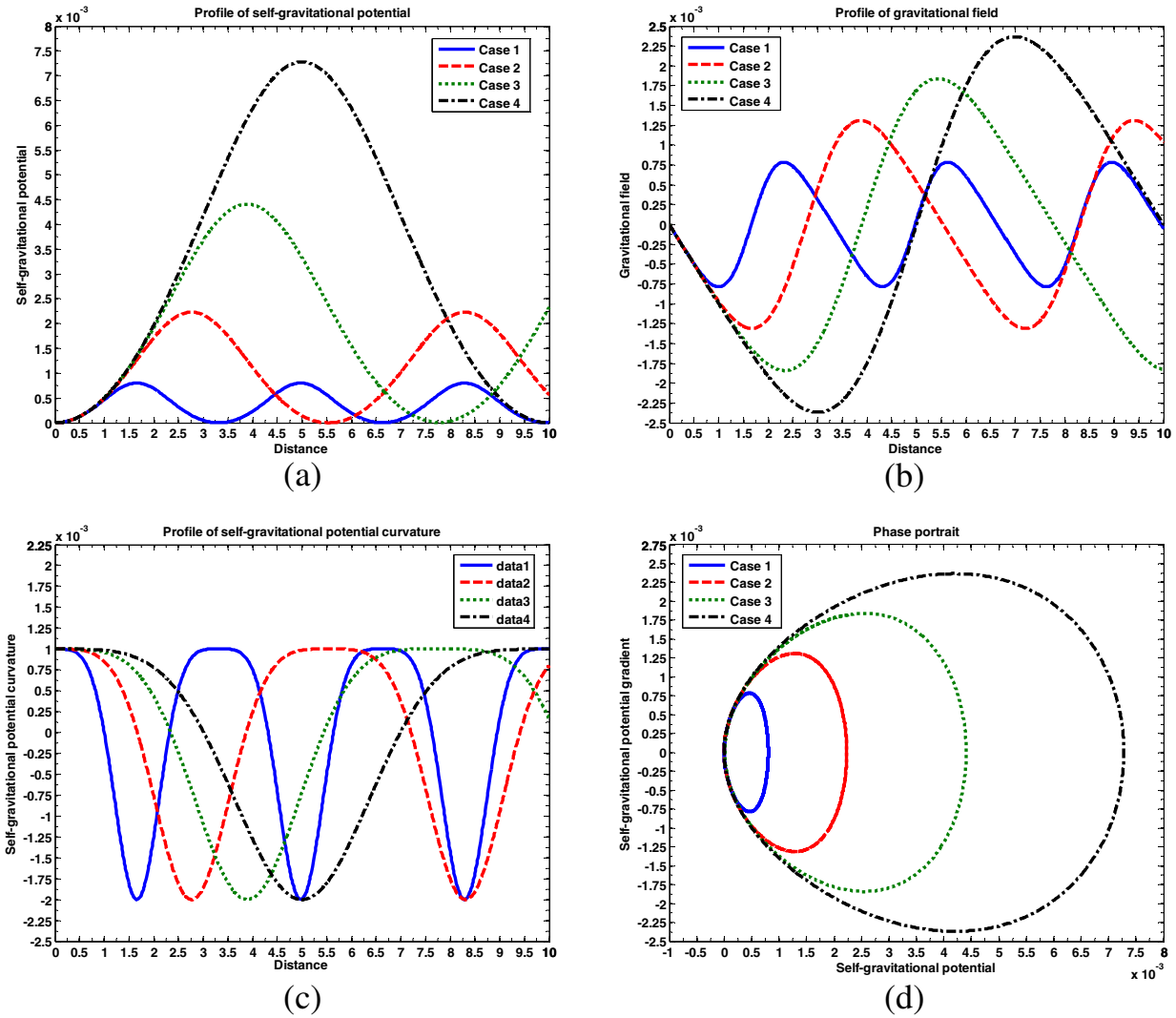

Fig. 5. Same as Figure 4, but with $m_d = 8.28 \times 10^{-12}$ kg. Various lines correspond to case (1): $\mu = 0.32$ (blue line), case (2): $\mu = 0.53$ (red line), case (3): $\mu = 0.74$ (green line), and case (4): $\mu = 0.96$ (black line), respectively.

obtained by multiscale analyses under the framework of the point-mass (Newtonian) and point-charge (Coulombic) approximations within the nonrelativistic limit of usual classical theory.

2. Various nonlinear eigenmode structures of the KdV-family like compressive (hump) solitons and soliton-chains as wide-range solitary spectral patterns are found to coevolve and co-propagate in such a system amidst small-amplitude approximation (weak nonlinearity and dispersion) within some judiciously chosen realistic plasma conditions.
3. The new eigenmode structures of the cloud are contributed by the collective gravito-electrostatic dynamics of the inertial species and thermal species amidst an integrated interplay of diverse nonlinear (hydrodynamic in origin), dispersive (self-gravitational in origin) and weakly dissipative (collisional in origin) effects.
4. The intrinsic conservative dynamics involved in the KdV systems is well satisfied in our model in spite of the inclusion of the grain-charge fluctuation and various collisions on the lowest-order perturbations in quasi-neutral hydrodynamic equilibrium configuration (due to closed structural form of various obtained phase portraits).
5. The proposed model investigation, although idealized in time-stationary regime, shows scopes for further improvement to understand the temporal evolution of the eigenmodes in presence of various spatio-temporal inhomogeneities in a more refined manner.
6. This is accentuated that the electrostatic eigenmodes have strengths comparable with those of the self-gravitational ones on common unit base of comparison (in terms of the plasma thermal potential). This, however, is legitimate for the grains which are not too huge, as their charge-to-mass ratios are too high to make the Coulomb and self-gravitational potentials, or forces fully comparable in strength. Grains exhibiting such characteristics normally reside in the inner part of the cloud, and hence, this comparison, in principle,

holds good for the internal denser region of the cloud structure under consideration.

7. The observed eigenmode signatures of the gravito-electrostatic origin, more particularly, different solitary spectral patterns and spectral transitions of the KdV-family of astrophysical importance, are in partial and qualitative correspondence with various multispace satellite observations, imaging detections and experimental laboratory findings with or without self-gravity reported so far in available literature [5–7,18–29]. Additionally, in laboratory scale too, such observational features of the nonlinear normal mode behavior in dust-contaminated plasmas are reported for existence in Q-machine devices under different conditions [30,31]. In such experimental findings, the most important dissipative processes behind shock-like structure formation are the charging of dust grains, the absorption of ions by grains, and the transfer of the ion momentum to the grains like in our proposed analyses.
8. For a more creative and comprehensive understanding of the evolving fluctuation dynamics, our model needs to be elaborated incorporating grain rotations, magnetic field, non-identical grains, diffusion, viscosity, grain-size distribution, etc. [14–24]. Exploration on the key processes behind how molecular cloud complexes are formed by accumulation of matter along magnetic flux tubes [24] may be an added future direction for further interesting study.
9. Moreover, our pulsational mode analyses based on the grainy Coulomb collisions in presence of grain-charge fluctuations may give rise to a new acceleration mechanism called *charge-fluctuation-induced acceleration* (in hydrodynamic approach), or *Fermi acceleration* (in magnetohydrodynamic formalism) in astrophysical plasma and space environments [23]. This novel mechanism is likely to affect the rate of grain flow, coagulation and shattering of the population density of small grains (radial size $\sim$0.10 μm). As per the law of conservation of energy, the new energy sources for this kind of acceleration mechanism come from the various irreversible plasma processes (triggered by the interaction of the electron and ion currents) occurring on the grain surfaces in the background plasma configuration.
10. Lastly and most importantly, although simplified and idealized, the adopted methodologies, strategic techniques and analyses may extensively be useful as the crucial role players in the form of input elements in further investigating the basic features of the self-gravitational collapse, formation and evolution of stars, galactic structures and other cluster-like astrophysical objects in different practical regimes of space and plasma environments.

The valuable comments, specific remarks and precise suggestions by the anonymous referees to refine the pre-revised original manuscript into the present post-revised improved form, are very gratefully acknowledged. Moreover, the financial support from the Department of Science and Technology (DST) of New Delhi, Government of India, extended to the authors through the SERB Fast Track Project (Grant No. SR/FTP/PS-021/2011) is also thankfully recognized.

References

1. F.H. Shu, F.C. Adams, S. Lizano, Ann. Rev. Astron. Astrophys. **25**, 23 (1987)
2. R.B. Larson, Rep. Prog. Phys. **66**, 1651 (2003)
3. R.S. Klessen, M.R. Krumholz, F. Heitsch, Adv. Sci. Lett. **4**, 258 (2011)
4. B.T. Draine, E.E. Salpeter, Astrophys. J. **231**, 77 (1979)
5. F. Verheest, Space Sci. Rev. **77**, 267 (1996)
6. F. Verheest, P.K. Shukla, Phys. Scr. **55**, 83 (1997)
7. T. Cattaert, F. Verheest, Astron. Astrophys. **438**, 23 (2005)
8. P.K. Karmakar, Pramana J. Phys. **76**, 945 (2011)
9. P.K. Karmakar, B. Borah, Phys. Scr. **86**, 1 (2012)
10. C.B. Dwivedi, A.K. Sen, S. Bujarbarua, Astron. Astrophys. **345**, 1049 (1999)
11. B.P. Pandey, J. Vranjes, S. Poedts, P.K. Shukla, Phys. Scr. **65**, 513 (2002)
12. F. Verheest, V.M. Cadez, Phys. Rev. E **66**, 056404 (2002)
13. J. Vranjes, B.P. Pandey, S. Poedts, Phys. Rev. E **64**, 066404 (2001)
14. A.A. Mamun, P.K. Shukla, IEEE Trans. Plasma Sci. **30**, 720 (2002)
15. U. de Angelis, Phys. Scr. **45**, 465 (1992)
16. A.A. Mamun, P.K. Shukla, Phys. Scr. **T98**, 107 (2002)
17. C. Cui, J. Goree, IEEE Trans. Plasma Sci. **22**, 151 (1994)
18. P.K. Shukla, B. Eliasson, Rev. Mod. Phys. **81**, 25 (2009)
19. A. Piel, A. Melzer, Plasma Phys. Control. Fusion **44**, R1 (2002)
20. F. Verheest, Phys. Scr. **T63**, 99 (1996)
21. S. Burman, A. Roy Chowdhury, Chaos Sol. Fract. **13**, 973 (2002)
22. V.E. Fortov, A.V. Ivlev, S.A. Khrapak, A.G. Khrapak, G.E. Morfill, Phys. Rep. **421**, 1 (2005)
23. A.V. Ivlev, A. Lazarian, V.N. Tsytovich, U. de Angelis, T. Hoang, G.E. Morfill, Astrophys. J. **723**, 612 (2010)
24. R.M. Crutcher, Ann. Rev. Astron. Astrophys. **50**, 29 (2012)
25. P.K. Karmakar, Res. Phys. **2**, 77 (2012)
26. Guo Zhi-Rong, Yang Zeng-Quiang, Yin Bao-Xiang, Sun Mao-Zhu, Chin. Phys. B **19**, 115203 (2010)
27. B.P. Pandey, J. Vranjes, S.V. Vladimirov, Phys. Plasmas **19**, 093701 (2012)
28. G. Jacobs, V.V. Yaroshenko, F. Verheest, Phys. Rev. E **66**, 026407 (2002)
29. A.V. Volosevich, C.-V. Meister, Contrib. Plasma Phys. **42**, 61 (2002)
30. S.I. Popel, T.V. Losseva, A.P. Golub, R.L. Merlino, S.N. Andreev, Contrib. Plasma Phys. **45**, 461 (2005)
31. J.E. Thomas, Contrib. Plasma Phys. **49**, 316 (2009)
32. J. Vranjes, Astrophys. Space Sci. **213**, 139 (1994)